Compensation for time fluctuations of phase modulation in a liquid-crystal-on-silicon display by process synchronization in laser materials processing

Compensation for time fluctuations of phase modulation in a liquid-crystal-on-silicon display by process synchronization in laser materials processing

Rainer J. Beck,* Jonathan P. Parry, Jonathan D. Shephard, and Duncan P. Hand

Applied Optics and Photonics Group, School of Engineering and Physical Sciences, Heriot-Watt University, Edinburgh, EH14 4AS, UK

*Corresponding author: rjb8@hw.ac.uk

Received 29 November 2010; revised 18 April 2011; accepted 19 April 2011; posted 22 April 2011 (Doc. ID 138760); published 13 June 2011

We demonstrate the adverse influence of temporal fluctuations of the phase modulation of a spatial light modulator (SLM) display device on nanosecond laser micromachining. We show that active cooling of the display reduces the amplitude of these fluctuations, and we demonstrate a process synchronization technique developed to compensate for these fluctuations when applying the SLM to laser materials processing. For alternative SLM devices developed specifically for laser wavefront control (which do not exhibit such flickering problems), we show that our process synchronization approach is also beneficial to avoid machining glitches when switching quickly between different phase profiles (and hence beam patterns). © 2011 Optical Society of America

OCIS codes: 050.1970, 140.3390, 230.6120.

1. Introduction

Spatial light modulators (SLMs) based on liquid-crystal microdisplays are powerful devices for beam shaping due to their very high spatial resolution, their direct programmability and their speed. Numerous papers have been published on applications of SLMs as programmable lenses and filters [1], optical tweezers [2,3], focus tracking in confocal microscopy [4], and beam shaping for femtosecond [5,6] and picosecond [7] laser machining. We demonstrated recently the successful application of the SLM LC-R 2500 manufactured by Holoeye for beam shaping in nanosecond laser materials processing [8]. This device has the advantage of being based on a standard SLM display. Cooling the display by heat sinking allowed it to cope with the high average powers required for standard nanosecond laser machining. Incorporating an active beam-shaping element such as an SLM into a laser machining workstation adds increased flexibility and the potential of process control, the driver for the work presented in this paper.

The phase modulation of the Holoeye device exhibits inherent time fluctuations as analyzed by Lizana *et al.* [9,10] due to the electrical addressing of the display. Such standard SLM display devices are typically addressed by a pulse-width-modulated signal, resulting in a temporal variation of the voltage applied to each pixel of the display [11,12]. The fluctuations that result are not observed by the human eye, and so this is not a problem when used as a display. However, when applying SLMs to laser micromachining with pulse repetition rates a few orders of magnitude higher than the frequency of the flickering, these fluctuations can adversely affect the machining outcome as we demonstrate in this paper (Subsection 2.A). We show that active cooling of the display of the SLM reduces the amplitude of the flickering (Subsection 2.C). More usefully, we report our

0003-6935/11/182899-07$15.00/0

development of a process synchronization technique between the graphics card controlling the SLM and the laser machining workstation to compensate for the inherent flickering (Subsection 2.D).

A second commercially available SLM, the LCOS-SLM X10468 from Hamamatsu, was investigated in the context of temporal fluctuations of the phase response. This device does not exhibit flickering; however, for laser machining processes where the SLM is switched between different phase profiles during the actual laser machining, the process synchronization approach can still be applied to improve the quality of the outcome, as described in Subsection 3.C.

2. Experimental Results with the Holoeye SLM

A. Setup

The SLM LC-R 2500 manufactured by Holoeye operates in reflection with XGA resolution (1024 × 768 pixels) on a display size of 19.5 mm × 14.6 mm. The image frame rate is 75 Hz with 256 available gray values for each pixel. According to the manufacturer, the pixel pitch is 19 μm and the fill factor is >93%. The device was incorporated into our nanosecond laser machining workstation, a Nd:YVO_4 system (Spectra-Physics Inazuma). The wavelength of the laser is 532 nm with a pulse length of ~65 ns and an available repetition rate of 15–100 kHz. Linearly polarized light, expanded using a telescope, is incident on the SLM close to normal incidence (see Fig. 1). Using a 6-f system consisting of a telescope arrangement and the flat field lens of the galvanometric (galvo) scanhead system, the beam is focused onto the workpiece. As described in our previous publication [8], the SLM display is attached to a custom-designed copper mount for cooling to enable the application for high average power nanosecond laser pulses. The copper mount acts as a passive heat sink with an option for additional water cooling.

The display of the SLM uses a 45° twisted nematic liquid-crystal layer. Different configurations regarding the polarization state and angle of the incident light are suggested in the literature in order to achieve a phase-only or phase-mostly configuration of this device [2,9,13]. These normally use a polarizing element as an analyzer after the SLM. Standard nanosecond laser machining applications require a relatively high average power at the workpiece. Consequently, the system was configured to have linearly polarized light incident on the SLM at an angle of 10° but no analyzer after the SLM in order to avoid further loss of laser intensity on the workpiece. The look-up table of the SLM, determining the relationship between the addressed gray value and the resulting electric field across the liquid crystal, has been recalibrated using an interferometric calibration method [14]. Using this technique, a fairly linear phase response between 0 and 2π can be achieved for a wavelength of 532 nm, as shown in [8].

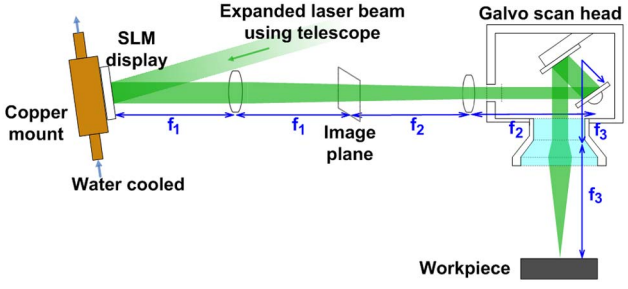

Fig. 1. (Color online) Setup of SLM embedded into laser machining workstation.

B. Effect of Flickering on Laser Micromachining

In order to determine the temporal beam shaping response of the SLM, a high-speed camera (Kodak 4502 m) was placed close to the focus of the optical system to monitor the spatial intensity distribution of the laser pulses. For this purpose, the laser beam was highly attenuated by means of a beam splitter with a splitting ratio independent of the orientation of the polarized light and additional neutral-density filters. The laser repetition rate was set to 40.5 kHz, the maximum frame rate of the high-speed camera was 40.5 kHz, and the shutter time was much longer than the pulse length of the laser, which allowed the spatial intensity distribution of single laser pulses to be investigated. For the measurement, a binary grating with a phase difference of 0.8π was addressed constantly to the SLM. This phase difference results in similar intensities for the zero order and the first diffraction orders of the laser beam and was chosen to emphasize the impact of the zero-order flickering. Each spot on the high-speed camera, which was positioned slightly off focus, had a diameter of ~15 pixels. The average intensity of a 20-pixel-diameter area for each spot has been determined in software as a measure for the intensity. As shown in Fig. 2, the intensities of the zero order and of the first diffraction orders vary significantly with time, despite the binary grating being addressed continuously to

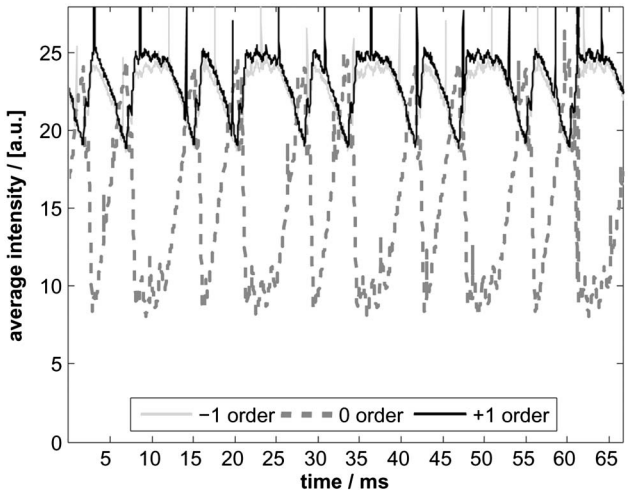

Fig. 2. Fluctuations of intensities of zero and first diffraction orders due to flickering of the SLM (temperature of display 24 °C).

the SLM. The temperature of the SLM display was 24 °C, measured using a pyrometer. The frequency of the periodic fluctuations is determined to be 75 Hz (period ~13 ms) corresponding to the frequency of the graphics cards. In addition to that, there is a subfluctuation with a frequency of about 150 Hz (period ~7 ms). Indeed, it is the pulse-width-modulated signal from the control electronics used to drive the pixels of the SLM display that gives rise to these fluctuations, also referred to as flickering, as reported by Lizana *et al.* [9,10] and Hermerschmidt *et al.* [11]. This can be a significant problem for the application of such an SLM for beam shaping in laser machining, in particular with laser repetition rates typically being a few orders of magnitude higher than the frequency of the flickering. The narrow peaks appearing in the intensity plot in Fig. 2 are probably artifacts due to the laser and the high-speed camera using different clocks with possibly a slightly different frequency around 40.5 kHz. The intensity values for the first diffraction orders are slightly different. This is caused by a consistent experimental error due to taking a point measurement within a finite size spot on the high-speed camera.

In order to investigate the impact of this flickering on the outcome of the laser machining processes, the binary grating described above was addressed continuously to the SLM. Using a galvo scan head system (see Fig. 1), the resulting three spots for the zero order and first diffraction orders are scanned perpendicularly at a speed of 12.5 mm/s across the workpiece surface, in this case a metal-coated glass slide. The laser power was adjusted to be just above the ablation threshold of the metal. The machining result [Fig. 3(a)] exhibit clear periodic variations with a periodicity that can be associated with the flickering of the SLM at 75 Hz. The quality of the laser machining process is hence clearly affected by the flickering of the display. Comparing the machining result in Fig. 3(a) with the intensity data in Fig. 2, an ablation threshold of 22 [a.u.] can be estimated. This value is then used, together with the intensity data, to simulate the expected machining [Fig. 3(b)]. The predictions are a close approximation to the experimental result.

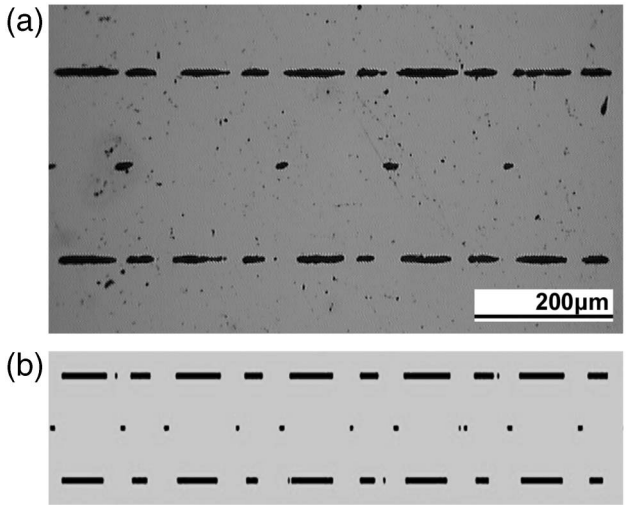

Fig. 3. (a) Laser machining using the scan head (scanning direction left to right, speed 12.5 mm/s) of metal-coated glass slide with binary grating addressed to SLM and (b) modeled machining results based on data shown in Fig. 2.

C. Temperature Dependence of Flickering

The experiments described in Subsection 2.B were repeated but this time while varying the SLM temperature. With the results presented in Subsection 2.B, the copper mount to which the SLM is attached was simply acting as a passive heat sink, and no additional water cooling was used. Additional cooling is likely to be useful, however, in order to reduce the amplitude of the inherent flickering of the SLM as described in Subsection 2.B. The intensity distribution when using the same binary grating as before was measured again by means of the high-speed camera (frame rate 40.5 kHz) with a laser repetition rate of 40.5 kHz but in this case for various SLM display temperatures. The display temperature was controlled using a closed-loop water cooling and heating unit. Figure 4(a) shows the dependence of the maximum and the minimum intensity values of the zero and the first diffraction orders on the display temperature, measured using a pyrometer. Figure 4(b) shows the amplitude of the flickering, i.e., the difference between the maximum and minimum intensity values for the zero and the first diffraction orders. It can be seen that cooling the device to a temperature of 17 °C significantly reduces the amplitude of the flickering compared to a temperature of 39 °C. The amplitude of the flickering of the zero order, for example, is reduced by ~50%, from ~25 [a.u.] to ~13 [a.u.]. Display temperatures of around 40 °C are typically reached when having the laser at full power (i.e., 14.7 W) incident on the SLM over a timescale of tens of minutes with the copper mount acting as a passive heat sink without water cooling.

This temperature dependence of the flickering can be explained by temperature-induced changes in the viscosity of the liquid crystals. The viscosity determines the response of the liquid crystals to changes of the applied electric field, driven by the pulse-width-modulated signal. So for lower temperatures, the liquid-crystal layer is “less sensitive” to changes due to the electronic addressing of the display. The liquid-crystal-on-silicon (LCoS) display used in this SLM is manufactured by Philips (Model X97c3A0) and contains 45° twisted nematic liquid crystals. We were not able to obtain information regarding the molecular constituents of the liquid crystal; also, information about the viscosity and especially the rotational viscosity coefficient of this particular liquid crystal was not available. This prevents a more detailed explanation of the measured linear dependence of the amplitude of the flickering on the temperature as shown in Fig. 4. In general, the viscosity increases at lower temperatures due the lower

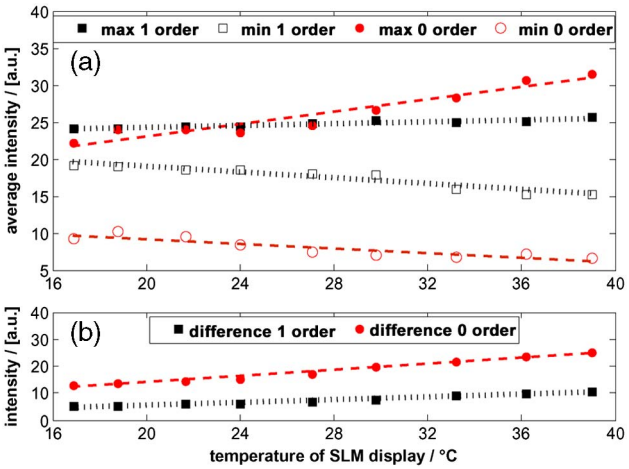

Fig. 4. (Color online) Temperature dependence of flickering for zero and first diffraction order intensities: (a) maximum and minimum intensity values for flickering and (b) difference between the maximum and minimum values.

molecular kinetic energy [15]. According to an empirical rule, for every temperature rise of 10°–15°, the rotational viscosity decreases by a factor of 2 [16]. Further cooling of the device is limited by the dew point of the ambient air. For lower temperatures, water condensation at the cover glass of the display will occur and in combination with a high- power laser beam could potentially damage the SLM display.

D. Process Synchronization to Compensate for Flickering

As presented above, cooling can be used to significantly reduce the amplitude of the flickering for an SLM with a pulse-width-modulated control signal, though it cannot fully be prevented. Thus, we developed a process synchronization technique between the graphics card controlling the SLM and the nanosecond laser machining workstation in order to block the laser beam and stop the galvo motion during the flicker and thus prevent unwanted machining. The basic idea is to trigger the shutter of the laser and the galvo scanhead system with a delayed signal from the graphics card based on previous measurement and analysis of the flickering process. For this purpose, the vertical sync pulse of the graphics card, defining the start of a new frame, is extracted from the graphics card and used as trigger signal for a pulse generator. The custom output signal from the pulse generator is connected to an optically isolated I/O input of the control unit of the scan head system in order to externally trigger the laser machining workstation. The results when machining stainless steel at a scan speed of 40 mm/s having again a binary grating addressed to the SLM are shown in Fig. 5(a) or the normal and unsynchronized process and Fig. 5(b) using the process synchronization technique. For the latter result [Fig. 5(b)], the laser-machined lines arising from the first diffraction orders are continuously black, implying similar beam intensities when scanning the beam across the work piece. The impact of the zero order can

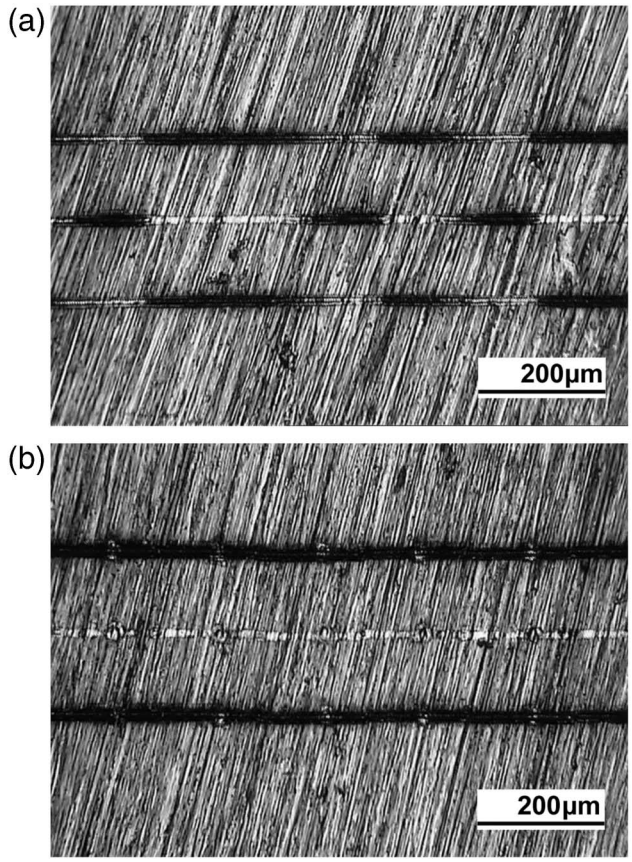

Fig. 5. (Color online) Machining result after scanning a laser beam modulated by a constant binary grating at a speed of 40 mm/s across stainless steel: (a) without and (b) with flickering compensation using process synchronization.

therefore be significantly reduced. The remaining energy in the zero order is causing some visible melting at the surface of the work piece. It should be noted, however, that for this experiment, the shutter of the laser was open and the scan head system moving for only 40% of every frame of the graphics card and, respectively, the SLM, so the removal of flickering in order to improve the quality of the laser machining for this particular case is associated with an increased processing time by a factor of 2.5.

3. Experimental Results with the Hamamatsu SLM

A. Setup

The experimental configuration for the Hamamatsu LCOS-SLM X10468-04 is essentially the same as that described in Subsection 2.A except that the SLM is replaced and the laser beam diameter was reduced slightly using an aperture to match the dimensions of the display (16 mm × 12 mm). The half-wave plate is altered to generate a linear polarization that results in a phase only modulation for this device, which has linear nematic liquid crystals. The display has a SVGA resolution (800 × 600 pixels) with a fill factor of 95%, and the frame rate is 60 Hz with 256 available gray values for each pixel. The Hamamatsu X10468-04 employs analog driving. The refresh rate

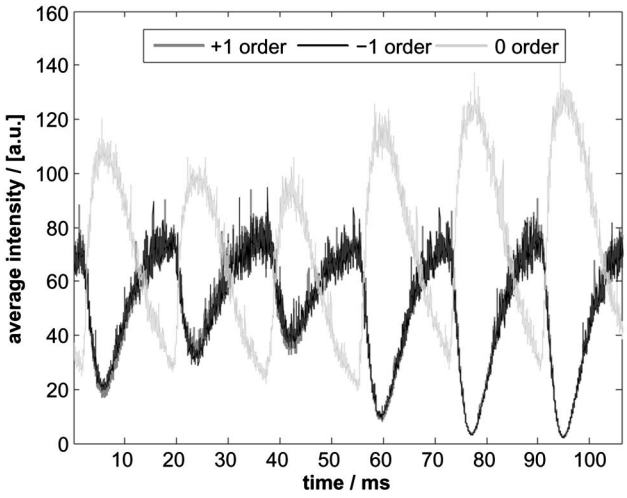

Fig. 6. Periodic variation of intensities of the zero order and first diffraction orders when alternating on a single-frame basis between two similar binary gratings addressed to the SLM. The first diffraction orders are almost identical.

is 480 Hz, and the alternate refresh rate is 240 Hz [17]. This device has a high-reflectivity dielectric coating, designed for a wavelength of 532 nm, between the liquid-crystal layer and the driving electronics. Thus, the display is better able to cope with the laser powers of our nanosecond system, and no additional cooling is required.

B. Response of the Spatial Light Modulator for Changes on a Single-Frame Basis

The measurement of potential flickering is carried out according to Subsection 2.B. No significant fluctuations of the phase modulation of the device could be observed in this case, and also no obvious effect was found on the outcome of laser machining when moving the diffracted laser beam across the workpiece with a laser power close to the ablation threshold of the material.

The big advantage of SLM devices compared to fixed optics, such as gratings or diffractive optical elements for beam shaping applications in laser machining, is the potential to change between different phase profiles "on-the-fly," i.e., during the actual machining process. In this context, the response of the SLM when alternating between different binary gratings every frame was measured using a similar arrangement to that described in Subsection 2.B, i.e., by means of the high-speed camera with a frame rate of 40.5 kHz and a laser repetition rate of 40.5 kHz. For simplicity, two binary gratings were chosen, having the same periodicity (i.e., 20 pixels) and phase difference (i.e., 0.8π; pixel gray values 100 and 0) but shifted by half the periodicity relative to each other. These gratings, although different, generate identical spatial intensity distributions at the focus of the system and thus make it easier to analyze the data from the high-speed camera. Each spot for the first diffraction orders and the zero order on the sensor of the camera had a diameter of ~10 pixels. The average intensity of a 16-pixel-diameter area for each spot has been determined in software as a measure for the intensity. Figure 6 shows the temporal variations of the intensities of the zero and the first diffraction orders when changing between the two binary gratings on a single-frame basis. The finite response time of the SLM display, mainly caused by the viscosity of the liquid-crystal layer, is the cause of this behavior.

C. Process Synchronization to Compensate Finite Response Time

In order to determine the response time for an actual machining process, two binary gratings having a phase difference of 0.8π as before but different periodicities (20 and 10 pixels) were alternately addressed (frame by frame) to the SLM. The angle of diffraction was thus switched on a frame-by-frame basis. The laser beam is scanned perpendicular to the orientation of the diffraction spots at a speed of

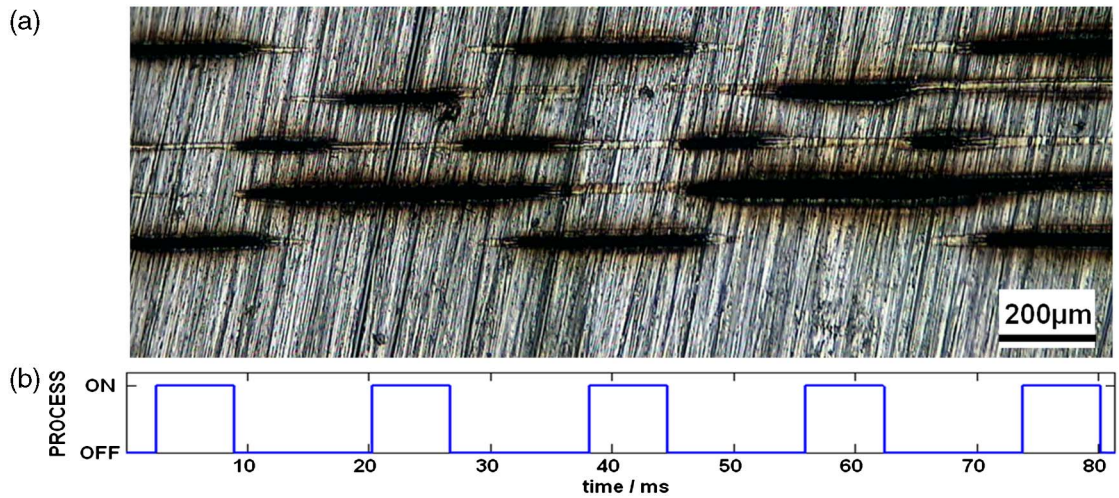

Fig. 7. (Color online) (a) Machining result when alternating between two binary gratings with different periodicities on the SLM while scanning the laser beam at a speed of 25 mm/s across stainless steel (scanning direction from left to right) and (b) schematic for synchronization technique indicating when the process is "on" and "off."

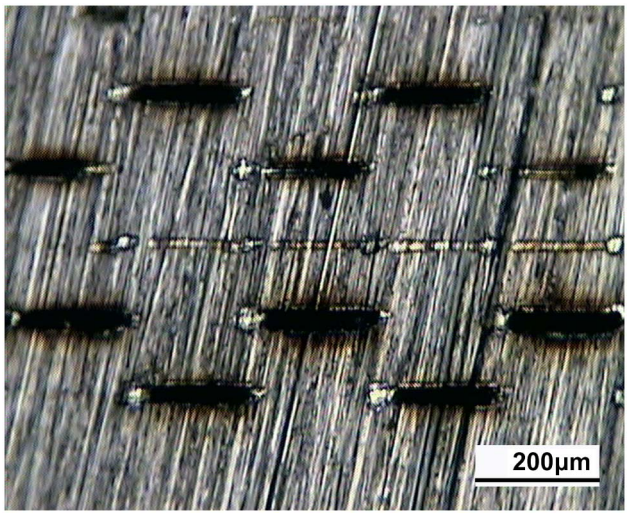

Fig. 8. (Color online) Machining result with settings as described in Fig. 7 but using the process synchronization technique.

25 mm/s across a stainless steel sample by means of the galvo scanhead. The laser machining outcome (laser repetition rate: 40.5 kHz, average power ~11 W) is shown in Fig. 7(a). The outermost pairs of parallel marks correspond to the 10 pixel period grating, while the more closely spaced pairs of marks correspond to the 20 pixel period grating. However, there are a series of marks in the center, in addition to the desired marks, associated with a strong zero-order beam appearing periodically whenever the grating pattern is being addressed to the SLM changes.

As before, the process synchronization technique can be applied in order to block the laser beam whenever its spatial intensity distribution is inappropriate for a particular laser machining application. The vertical sync signal from the graphics card is extracted, and a pulse based on analysis of the intensity data shown in Fig. 6 is generated in order to control the laser machining workstation. In this case, machining is stopped whenever the intensity of the zero order exceeds that of the first diffraction orders, as indicated in Fig. 7(b). The laser machining result when using this process synchronization technique and the same laser parameters as before are shown in Fig. 8. The deep, blackened laser marks resulting from the zero-order laser beam are no longer present. Also, all the marks resulting from the first diffraction orders are of roughly the same length.

4. Conclusion

The use of an SLM for beam shaping is a powerful technique in laser machining. However, a conventional SLM display with a standard pulse-width-modulated signal (such as the LC-R 2500) exhibits temporal fluctuations of its phase modulation. We have demonstrated that this flickering can have a significant adverse effect on the outcome of short-pulsed and high-repetition-rate laser machining. However, we have also demonstrated techniques to reduce the impact of this flickering: first reducing its amplitude by active cooling of the device and second by implementing a process synchronization technique between the laser machining workstation and the graphics card controlling the SLM. Although SLM devices designed specifically as laser wavefront modulators do not exhibit the same flickering problems as standard display devices, if changes to phase patterns are required during processing, transition effects can occur, resulting in unintended machining. We have demonstrated that a similar process synchronization technique can be used to successfully prevent unwanted machining. Overall, the SLM in combination with an appropriate control system offers increased flexibility and improved process control for the laser machining workstation.

This work was partly funded by the UK Engineering and Physical Sciences Research Council, (EPSRC) (IMRC EP/F02553X). A special thanks to our industrial collaborator Renishaw plc for their funding and support. The authors are grateful to Hamamatsu Photonics, via Doctor Raymond Livingstone, for their support and the loan of their device for our research.

References

1. M. J. Yzuel, J. Campos, A. Marquez, J. C. Escalera, J. A. Davis, C. Lemmi, and S. Ledesma, "Inherent apodization of lenses encoded on liquid-crystal spatial light modulators," Appl. Opt. **39**, 6034–6039 (2000).
2. M. Reicherter, S. Zwick, T. Haist, C. Kohler, H. Tiziani, and W. Osten, "Fast digital hologram generation and adaptive force measurement in liquid-crystal-display-based holographic tweezers," Appl. Opt. **45**, 888–896 (2006).
3. E. Martin-Badosa, M. Montes-Usategui, A. Carnicer, J. Andilla, E. Pleguezuelos, and I. Juvells, "Design strategies for optimizing holographic optical tweezers set-ups," J. Opt. A **9**, S267–S277 (2007).
4. A. J. Wright, B. A. Patterson, S. P. Poland, J. M. Girkin, G. M. Gibson, and M. J. Padgett, "Dynamic closed-loop system for focus tracking using a spatial light modulator and a deformable membrane mirror," Opt. Express **14**, 222–228 (2006).
5. L. Kelemen, S. Valkai, and P. Ormos, "Parallel photopolymerisation with complex light patterns generated by diffractive optical elements," Opt. Express **15**, 14488–14497 (2007).
6. Z. Kuang, D. Liu, W. Perrie, S. Edwardson, M. Sharp, E. Fearon, G. Dearden, and K. Watkins, "Fast parallel diffractive multi-beam femtosecond laser surface micro-structuring," Appl. Surf. Sci. **255**, 6582–6588 (2009).
7. D. Liu, Z. Kuang, S. Shang, W. Perrie, D. Karnakis, A. Kearsley, M. Knowles, S. Edwardson, G. Dearden, and K. Watkins, "Ultrafast parallel laser processing of materials for high throughput manufacturing," in *Proceedings of LAMP 2009—The 5th International Congress on Laser Advanced Materials Processing* (Japan Laser Processing Society, 2009), paper 09-021.
8. R. J. Beck, J. P. Parry, W. N. MacPherson, A. Waddie, N. J. Weston, J. D. Shephard, and D. P. Hand, "Application of cooled spatial light modulator for high power nanosecond laser micromachining," Opt. Express **18**, 17059–17065 (2010).
9. A. Lizana, I. Moreno, A. Marquez, C. Iemmi, E. Fernandez, J. Campos, and M. J. Yzuel, "Time fluctuations of the phase modulation in a liquid crystal on silicon display: characterization and effects in diffractive optics," Opt. Express **16**, 16711–16722 (2008).

10. A. Lizana, A. Marquez, I. Moreno, C. Iemmi, J. Campos, and M. J. Yzuel, "Wavelength dependence of polarimetric and phase-shift characterization of a liquid crystal on silicon display," J. Eur. Opt. Soc. Rapid Publ. **3**, 08012 (2008).
11. A. Hermerschmidt, S. Osten, S. Krüger, and T. Blümel, "Wave front generation using a phase-only modulating liquid-crystal-based micro-display with HDTV resolution," Proc. SPIE 6584, 65840E (2007).
12. J. R. Moore, N. Collings, W. A. Crossland, A. B. Davey, M. Evans, A. M. Jeziorska, M. Komarcevic, R. J. Parker, T. D. Wilkinson, and H. Xu, "The silicon backplane design for an LCOS polarization-insensitive phase hologram SLM," IEEE Photon. Technol. Lett. **20**, 60–62 (2008).
13. J. Andilla, E. Martin-Badosa, and S. Vallmitjana, "Prediction of phase-mostly modulation for holographic optical tweezers," Opt. Commun. **281**, 3786–3791 (2008).
14. J. Oton, P. Ambs, M. S. Millan, and E. Perez-Cabre, "Multipoint phase calibration for improved compensation of inherent wavefront distortion in parallel aligned liquid crystal on silicon displays," Appl. Opt. **46**, 5667–5679 (2007).
15. P. Yeh and G. Claire, *Optics of Liquid Crystal Displays* (Wiley, 1999).
16. J. H. Lee, D. N. Liu, and S. T. Wu, *Introduction to Flat Panel Displays*, 1st ed. (Wiley, 2008).
17. Hamamatsu Photonics K. K., *LCOS-SLM X10468 Series—LC Driving System* (2010).